Effective Microwave Surface Impedance of Superconducting Films in the Mixed State

Chien-Jang Wu and Tseung-Yuen Tseng, *Senior Member, IEEE*

***Abstract*—The effective microwave surface impedance of multilayer structures made of high-T_c superconducting films in the mixed state, lossy dielectrics, and normal metals are theoretically calculated. The linear response of the superconductor to a microwave field is analyzed within both transmission line theory and the framework of self-consistent treatment of vortex dynamics reported by Coffey and Clem [18]. The microwave properties are investigated as a function of static field and film thickness for nonresonant structures. The effect of substrate thickness on the resonant phenomenon is carefully studied as well. Numerical results reveal that the substrate resonance in the Meissner state behaves like a parallel lumped-parameter resonantor, while in the vortex state it behaves as a series lumped resonant circuit. The basic distinction suggests that care should be taken in microwave applications when using superconducting films in the vortex state.**

***Index Terms*—Microwave surface impedance, mixed state, resonant phenomenon, superconducting films.**

NOMENCLATURE

Z_s	Surface impedance (defined as $Z_s \equiv R_s + jX_s$).
R_s	Surface resistance.
X_s	Surface reactance.
ω	Angular frequency.
f	Linear frequency.
μ	Permeability of the material.
$\tilde{\sigma}$	AC conductivity (defined as $\tilde{\sigma} \equiv \sigma' - j\sigma''$).
Z_{eff}	Effective surface impedance (defined as $Z_{\text{eff}} \equiv R_{\text{eff}} + jX_{\text{eff}}$).
T_c	Transition temperature of superconductor.
T	Temperature.
γ	Propagation constant in superconductor (defined as $\gamma \equiv j\tilde{k} \equiv \alpha + j\beta$).
$\tilde{k}$	Complex wavenumber in superconductor (defined as $\tilde{k} \equiv k' - jk''$).
α	Attenuation constant in the superconductor.
β	Phase constant in the superconductor.
λ_{ac}	Complex penetration depth (defined as $\lambda_{ac} \equiv \lambda' - j\lambda''$).
λ	Temperature and field dependence of penetration depth.
λ_0	London penetration depth at $T = 0$.
t	Reduced temperature (defined as $t \equiv T/T_c$).
B	Static magnetic field.
B_{c2}	Temperature dependence of upper critical field.
$B_{c2}(0)$	Upper critical field at $T = 0$.
δ_{nf}	Normal-fluid skin depth.
δ_n	Normal-state skin depth.
ρ_{nf}	Normal-fluid resistivity.
ρ_n	Normal-state resistivity.
$\tilde{\delta}_{vc}$	Effective skin depth due to vortex motion.
$\tilde{\rho}_v$	Effective resistivity due to vortex motion.
ϕ_0	Flux quanta.
$\tilde{\mu}_v$	Dynamic mobility due to vortex motion.
η	Viscous drag coefficient.
ρ_f	Flux-flow resistivity (defined as $\rho_f \equiv \rho_n B/B_{c2}(T)$).
κ_p	Temperature-dependent restoring force constant of pinning potential.
κ_{p0}	Restoring force constant of pinning potential at $T = 0$.
I_1	Modified Bessel function of the first kind of order one.
I_0	Modified Bessel function of the first kind of order zero.
U_0	Barrier height of pinning potential.
k_B	Boltzmann constant.
Z_1	Wave impedance of the superconductor.
d	Thickness of superconducting film.
h	Thickness of the dielectric substrate.
Z_0	Wave impedance of the vacuum.
ε	Relative permittivity of the dielectric substrate (defined as $\varepsilon \equiv \varepsilon' - j\varepsilon''$).
$\varepsilon(T)$	Temperature dependence of the relative permitivity of $SrTiO_3$.
$\tan\delta$	Loss tangent of the dielectric substrate (defined as $\tan\delta \equiv \varepsilon''/\varepsilon'$).
μ_0	Permeability of the vacuum.
ε_0	Permittivity of the vacuum.
b	Reduced static magnetic field (defined as $b \equiv B/B_{c2}(0)$).
Γ	Effective reflection coefficient.
S	Standing wave ratio.
γ_2	Propagation constant in the substrate (defined as $\gamma_2 \equiv \alpha_2 + j\beta_2$).
λ_2	Wavelength in the substrate (defined as $\lambda_2 \equiv 2\pi/\beta_2$).
k_2	Complex wavenumber of the substrate.
Z_2	Wave impedance of the substrate.
σ_m	Conductivity of the ground metal.
Z_3	Wave impedance of the ground metal.
l	Length of the transmission line.

Manuscript received April 30, 1996; revised October 16, 1996. This work was supported by the National Science Council of the Republic of China under Project NSC85-2112-M009-037PH.

The authors are with the Department of Electronics Engineering and The Institute of Electronics, National Chiao-Tung University, Hsinchu, Taiwan, R.O.C.

Publisher Item Identifier S 0018-9464(97)02087-6.

I. Introduction

THE DISCOVERY of high-temperature superconductors (HTSC's) has diversified their applications in the microwave regime. In designing microwave passive devices, such as filters [1], resonators [2], [3], and delay lines [4], the most important quantity in determining performance is the microwave surface impedance, $Z_s = R_s + jX_s$, of the superconductor. The surface resistance R_s indicates the dissipation, while the surface reactance X_s is related to the field screening in the superconductor. Measurements of surface impedance are widely used not only to determine the performance of the device but also to extract basic physics of the superconductor. As a fundamental aspect, the electron conduction mechanism can be better understood from the knowledge of Z_s according to the familiar two-fluid model [5]–[8].

The microwave surface impedance of the bulk sample is usually described as

$$Z_s = \sqrt{\frac{j\omega\mu}{\tilde{\sigma}}} \tag{1}$$

where ω is the angular frequency, μ the permeability of the material, and $\tilde{\sigma}$ the ac conductivity defined as $\tilde{\sigma} = \sigma' - j\sigma''$. Equation (1) is, in fact, the intrinsic surface impedance derived for a semi-infinite sample. However, single crystal samples utilized in microwave measurements are usually arranged in the shape of a platelet. A more relevant alternative for studying microwave properties is therefore the complex RF permeability instead of Z_s in (1). On the other hand, superconducting thin films are frequently used in microwave devices. Thus, the use of (1) is not adequate to investigate the microwave characteristics of a thin-film layered structure, the usual one conducted in the experiment. The structure is made of a superconducting film on a dielectric substrate with a ground metal such as copper or gold. Therefore, we must resort to the so-called effective microwave surface impedance, $Z_{\text{eff}} = R_{\text{eff}} + jX_{\text{eff}}$, which encompasses all possible material properties together with the thicknesses of the film and substrate. Besides, in the limit of infinite film thickness, Z_{eff} will naturally reduce to the intrinsic surface impedance. That is, if the thickness increases to some extent, the substrate will have no influence on Z_{eff} because it may be effectively shielded by the superconducting film.

To date, a great deal of investigation in effective microwave surface impedance has been theoretically and experimentally done. In the Meissner state, the film response to a microwave field is theoretically interpreted based on the well-known two-fluid theory and impedance transformation in transmission line theory [9]–[12]. For experimental data on the thickness-dependent Z_{eff}, we mention the papers of Oates *et al.* [13] and other work [14]–[17]. An interesting phenomenon shown in the above-described reports is the observation of the resonant behavior in effective surface resistance. Klein *et al.* [9] and Drabeck *et al.* [10], [11] have experimentally observed that the normal-state response exhibits a resonant behavior in the temperature-dependent surface resistance for high-T_c films deposited on the substrate $SrTiO_3$. Moreover, in the Meissner state, Hartemann [12] has also theoretically predicted the existence of substrate resonance phenomenon in the substrate-thickness-dependent effective surface resistance. At the substrate-resonance thickness, R_{eff} shows a peak, while X_{eff} makes an abrupt transition from maximum to minimum. The transition in X_{eff} is closely related to the ground bulk metal used at the backside of the substrate [12].

The electromagnetic propagation-dominated problems of type-II superconductors involving multilayer structures are also of interest and importance. The vortex dynamics can be investigated through the measurement of the vortex lattice response to microwave fields. The microwave field generates Lorentz forces on the vortices near the surface, which in turn causes an oscillation of vortices. These oscillating vortices will propagate into the interior of the superconductor under the influences of pinning and viscous forces. The intrinsic surface impedance, therefore, strongly relies on the vortex motion. A phenomenologically unified theory on Z_s of type-II superconductors has been developed by Coffey and Clem [18]–[20] with the method of self-consistent treatment of vortex dynamics where the effects of pinning, flux flow, and flux creep are incorporated. The electromagnetic transmission and reflection problem in type-II superconductors in the mixed state is then solvable on the basis of their theory [21]. Experimental verification on this propagation-dominated problem in a multilayer structure has been available from the work of Moser *et al.* [22]. According to the Coffey–Clem model, many investigators have studied the vortex dynamics by the measurements of surface impedance of high-T_c thin films [23]–[25]. The intrinsic surface impedance of type-II superconductors can be calculated via (1) if the ac conductivity is known. The development of the Coffey–Clem theory has clearly extended the attention on Meissner response to that in the mixed state. Therefore, we are motivated to specifically investigate the resonant phenomenon in the mixed state. The essential distinction of resonant behavior between Meissner and mixed states will be clearly illustrated in this paper. Some discussion on its physical argument is given as well.

Two layered structures will be studied in this work. One is the structure made of a superconducting film deposited on a semi-infinite lossy dielectric substrate. The other is the film on a substrate with finite thickness in addition to a gold ground plane. The superconducting thin film used in this study is the typical high-T_c superconductor, c axis oriented $YBa_2Cu_3O_{7-x}$ (YBCO). The substrates considered are MgO, $LaAlO_3$, or $SrTiO_3$, which are commonly utilized in microwave measurements.

II. Effective Surface Impedance of a Superconducting Film in the Mixed State

Let us first consider a superconducting thin film with thickness d deposited on the semi-infinite substrate, as depicted in the inset of Fig. 1. A uniform TE microwave field traveling in the $+x$ direction in vacuum impinges normally on a plane boundary with superconducting film at $x = 0$. A static magnetic field B is applied along the x direction to put the superconductor in the mixed state. The complex propagation constant in the superconducting film is $\gamma = j\tilde{k} = \alpha + j\beta$,

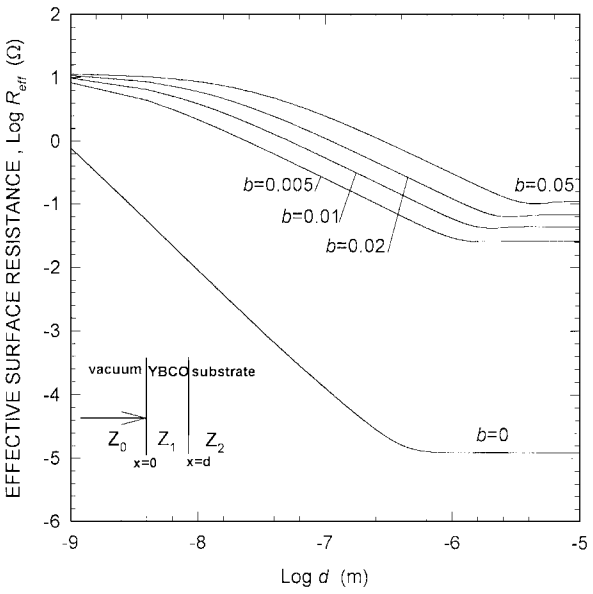

Fig. 1. The thickness-dependent effective surface resistance in (5) at various reduced static fields, $b = 0, 0.005, 0.01, 0.02$, and 0.05. The material parameters used are given in the text. The substrate is $SrTiO_3$.

where the real part, α, is the attenuation constant, and β is the phase constant. Based on the Coffey–Clem model [21], the complex wavenumber is $\tilde{k} = k' - jk'' = -j/\lambda_{ac}$, where the complex penetration depth λ_{ac} is expressed as

$$\lambda_{ac} \equiv \lambda' - j\lambda'' = \left[\frac{\lambda^2 - (j/2)\delta_{vc}^2}{1 + 2j\lambda^2\delta_{nf}^{-2}}\right]^{1/2} \tag{2}$$

where λ is the temperature and magnetic field dependent penetration depth, $\lambda = \lambda_0(1-t^4)^{-1/2}(1 - B/B_{c2}(T))^{-1/2}$ where λ_0 is the London penetration depth at $T = 0, t \equiv T/T_c$ is the reduced temperature, and $B_{c2}(T) \equiv B_{c2}(0)(1-t^2)(1+t^2)^{-1}$ is the temperature dependent upper critical field, where $B_{c2}(0)$ is the upper critical field at $T = 0$. The normal-fluid skin depth $\delta_{nf} \equiv (2\rho_{nf}/\mu_0\omega)^{1/2}$ is related to the normal-state skin depth $\delta_n \equiv (2\rho_n/\mu_0\omega)^{1/2}$ by $\delta_{nf} = \delta_n/\sqrt{f(T,B)}$, where ρ_{nf} and ρ_n are the normal-fluid and normal-state resistivities, respectively, and $f(T,B) = 1 - (1-t^4)(1 - B/B_{c2}(T))$. The complex effective skin depth due to vortex motion is defined by $\delta_{vc}^2 \equiv 2\tilde{\rho}_v/\mu_0\omega$, where $\tilde{\rho}_v$ is the effective resistivity given by $\tilde{\rho}_v(\omega,B,T) = B\phi_0\tilde{\mu}_v(\omega,B,T)$, with the dynamic mobility expressed as [18]

$$\tilde{\mu}_v(\omega,B,T) = \frac{1}{\eta}\left[1 + \left[\frac{j\omega\eta}{\theta\kappa_p} + \frac{1}{I_0^2(z) - 1}\right]^{-1}\right]^{-1} \tag{3}$$

where ϕ_0 is the flux quanta, η is the viscous drag coefficient defined as $\eta \equiv B\phi_0/\rho_f$ with $\rho_f = \rho_n B/B_{c2}(T), \kappa_p$ is the restoring force constant of a pinning potential well given by $\kappa_p = \kappa_{p0}(1-t^2)^2$ and $\theta \equiv I_1(z)/I_0(z)$ where I_1, I_0 are the modified Bessel function of the first kind of order one and zero, respectively, and the argument $z \equiv U_0(B,T)/2k_BT$ (k_B is the Boltzmann constant) is dependent on the barrier height of the potential, $U_0(B,T) \equiv U(1-t)^{3/2}B^{-1}$. The material parameters for the YBCO system used in this study are $T_c = 91$ K, $U = 0.15$ eV $- T, \kappa_{p0} = 2.1 \times 10^4$ N/m, $\rho_n(T) = 1.1 \times 10^{-8}T + 2 \times 10^{-7}\ \Omega - m, \lambda_0 = 140$ nm. The temporal part of the electromagnetic field is assumed to be $e^{j\omega t}$ in this paper. The wave impedance Z_1 of the superconductor, therefore, is given by

$$Z_1(\omega,T,B) = \sqrt{\frac{j\omega\mu_0}{\tilde{\sigma}}} = j\omega\mu_0\lambda_{ac} \tag{4}$$

where the complex ac conductivity $\tilde{\sigma} = \sigma' - j\sigma'' = -j/\omega\mu_0\lambda_{ac}^2$ has been adopted. The effective surface impedance at the vacuum/superconductor interface, $x = 0$, can be directly calculated with the help of the impendance transformation. The result is

$$Z_{\text{eff}} \equiv R_{\text{eff}} + jX_{\text{eff}} = Z_1\frac{Z_2 + Z_1\tanh(j\tilde{k}d)}{Z_1 + Z_2\tanh(j\tilde{k}d)} \tag{5}$$

where Z_2 is the wave impedance in the dielectric substrate given by

$$Z_2 = \frac{Z_0}{\sqrt{\varepsilon'}}\left(1 + \frac{j}{2}\tan\delta\right). \tag{6}$$

In (6), the substrate has relative permittivity $\varepsilon = \varepsilon' - j\varepsilon''$ and the loss tangent $\tan\ \delta \equiv \varepsilon''/\varepsilon'$ and the wave impedance of vacuum is $Z_0 = \sqrt{\mu_0/\varepsilon_0} = 377\ \Omega$.

By taking $SrTiO_3$ as a subtrate, in Figs. 1 and 2 we have respectively plotted the R_{eff} and X_{eff} in (5) as a function of film thickness at various reduced static fields, $b \equiv B/B_{c2}(0)$, at fixed frequency 10 GHz and temperature 77 K. The permittivity of $SrTiO_3$ at 77 K is $\varepsilon = 1000 - j0.5$ [12] and $B_{c2}(0) = 112\,T$ is taken for YBCO. The calculated parameters for YBCO at 10 GHz, 77 K, and $b = 0.01$ are $\lambda = 207$ nm, $\sigma' = 1.73 \times 10^7$ S/m, $\sigma'' = 2.54 \times 10^6$ S/m, $k' = 7.67 \times 10^5\ m^{-1}$, $k'' = 8.88 \times 10^5\ m^{-1}$ and $Z_1 = 0.044 + j0.051$. As can be seen in Fig. 1, at $b = 0$, corresponding to the Meissner-state response, for a thickness greater than about 500 nm $(\log\ d \approx -6.3), R_{\text{eff}}$ is essentially a constant and the film behaves as a bulk material. That is, the effect of the substrate has been completely shielded by the film. This critical thickness is observed to increase as b increases. For example, at $b = 0.01$ the critical thickness for complete shielding is estimated to be 2500 nm, which is five times as large as that at $b = 0$. We can easily understand this from the complex penetration depth λ_{ac} in (2). Fig. 3 shows the magnitude of λ_{ac}, the real part λ', and the imaginary part λ'' as a function of reduced field. It clearly indicates that $|\lambda_{ac}|$ increases with increasing b; namely, the field penetration through the superconducting film becomes more considerable at larger b field. Accordingly, in order to shield the substrate, the film thickness should effectively get larger. One can also interpret this phenomenon from the viewpoint of transmission coefficient. According to the paper of Coffey and Clem [21], the transmission coefficient increases with increasing b at fixed temperature and frequency. The better candidate for effectively shielding the influence of substrate is, therefore, the thicker film. The above arguments are consistent with the results shown in Figs. 1 and 2. We also observe that the difference, $R_{\text{eff}}(b \neq 0) - R_{\text{eff}}(b = 0)$, is about one order of magnitude for a very thin film, say $d = 1$ nm, whereas it can reach five orders of magnitude at $b = 0.05$ for a thick film with $d = 10\ \mu$m.

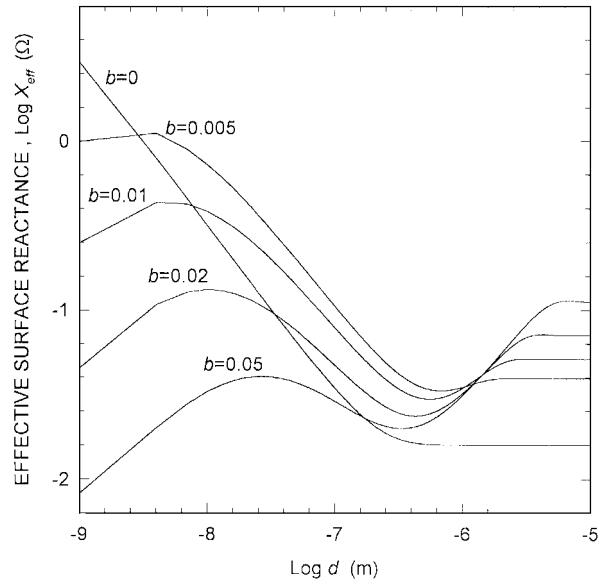

Fig. 2. The thickness-dependent effective surface reactance in (5) at various reduced static fields, $b = 0, 0.005, 0.01, 0.02$, and 0.05. The material parameters used are given in the text. The substrate is $SrTiO_3$.

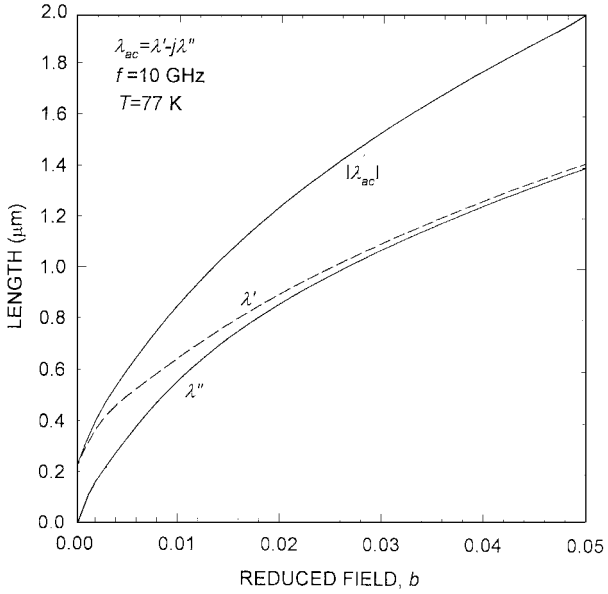

Fig. 3. The magnitude of complex RF penetration depth, $|\lambda_{ac}|$, imaginary and real parts of λ_{ac}, as a function of reduced static field at $f = 10$ GHz and $T = 77$ K. The material parameters used are typical of the high-T_c superconductor, YBCO.

Another interesting feature at $b \neq 0$ is the very different behavior in X_{eff} as illustrated in Fig. 2. The magnitude of discrepancy, $X_{\text{eff}}(b \neq 0) - X_{\text{eff}}(b = 0)$, increases with increasing b. Furthermore, the $X_{\text{eff}}(b \neq 0)$ initially increases with increasing film thickness and reaches a peak. The peak height then decreases with increasing b. Also there exists a valley before reaching the critical thickness of d. This peculiar behavior in X_{eff} will introduce an associated change in phase which is an important factor in microwave applications.

Some physical insight can be further gained from Fig. 3. At $b = 0$, the complex penetration depth λ_{ac}, is essentially a real number and, in fact, equals the London penetration depth λ.

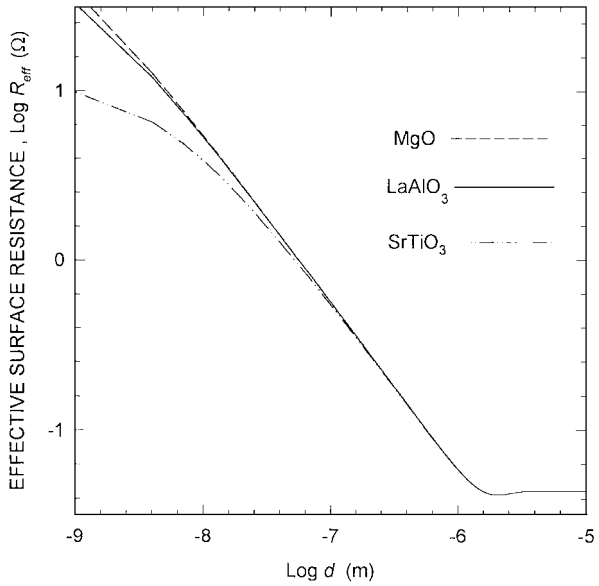

Fig. 4. The effective surface resistance in (5) versus film thickness for three substrate dielectrics at $f = 10$ GHz, $T = 77$ K, and $b = 0.01$. The permittivities of the dielectrics are given in the text.

This makes the conductivity $\tilde{\sigma}$ imaginary with $\tilde{\sigma} \approx -j\sigma'' = -j/\mu_0\omega\lambda^2$, a result of the conventional two-fluid model. In the two-fluid theory, the conductivity is expected to be $\tilde{\sigma} = \sigma' - j\sigma'' \approx -j\sigma''$, with the fact that $\sigma'' \gg \sigma'$. Moreover, the complex conductivity can be explicitly expressed in terms of the complex penetration depth and the result is

$$\sigma' = \frac{2}{\mu_0\omega}\frac{\lambda'\lambda''}{|\lambda_{ac}|^4}, \quad \sigma'' = \frac{1}{\mu_0\omega}\frac{(\lambda')^2 - (\lambda'')^2}{|\lambda_{ac}|^4}. \tag{7}$$

From Fig. 3 it is seen that the imaginary part λ'' is nearly equal to the real part λ' at larger values of b, which implies that the ac conductivity is approximately real according to (7). In this case, the response at 77 K and higher field is very similar to that of either a flux flow-dominated limit or simply the normal state. The investigation so far obviously encompasses all the previous studies, especially in the Meissner state [9]–[12], together with normal state [10]–[11]. Moreover, the effective reflection coefficient $\Gamma = (Z_{\text{eff}} - Z_0)/(Z_{\text{eff}} + Z_0)$ at the interface $x = 0$ can be evaluated, which is more convenient for analyzing the propagation-dominated problem for superconducting films in the mixed state. Meanwhile, one can readily determine the associated standing-wave ratio S, an important parameter in microwave engineering.

Fig. 4 illustrates the R_{eff} versus film thickness for various substrates at 77 K, 10 GHz, and $b = 0.1$. The permittivities of the substrates are $\varepsilon = 1000 - j0.5$ for $SrTiO_3$, $24 - j1.2 \times 10^{-4}$ for $LaAlO_3$, and $9.7 - j9.7 \times 10^{-6}$ for MgO. The effect of distinct substrates is considerable only for thinner films. However, there is nothing different in R_{eff} for these three substrates for thicker films. Also, the R_{eff} is basically the same for both $LaAlO_3$ and MgO. The results can be explained as follows. For a very thin film, say $d = 1$ nm, the substrate effect is pronounced for $SrTiO_3$ because of its high-loss tangent. The loss tangent of $LaAlO_3$ and MgO is about 10^{-6}, i.e., smaller than that of $SrTiO_3$ by two orders of magnitude.

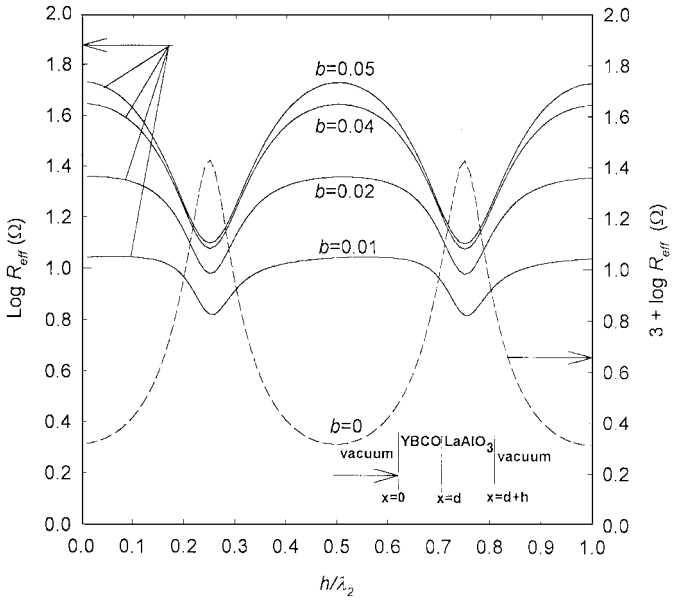

Fig. 5. The effective surface reactance in (9) as a function h/λ_2, at various reduced fields, $b = 0, 0.01, 0.02, 0.04$, and 0.05. λ_2 is the substrate wavelength in value of 6.1237 mm at $T = 77$ K and $f = 10$ GHz. The substrate is $LaAlO_3$. The material parameters used are described in the text.

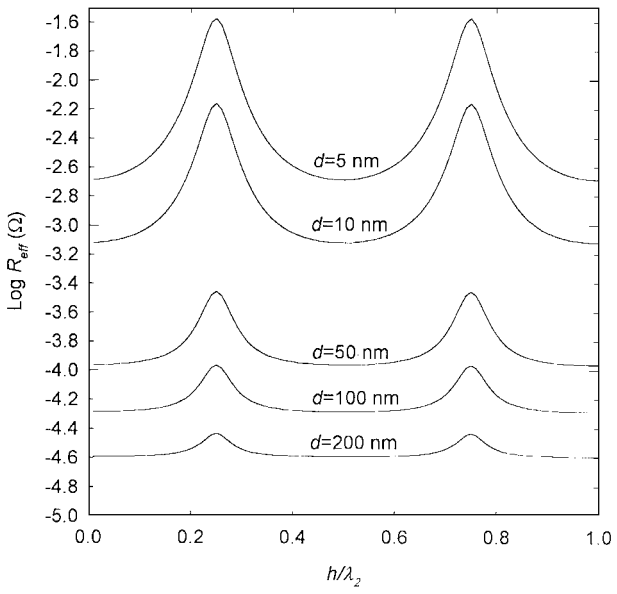

Fig. 6. The effective resistance in (9) versus h/λ_2 for various film thickness, $d = 5$ nm, 10 nm, 50 nm, 100 nm, and 200 nm, at $T = 77$ K, 10 GHz, and $b = 0$. $\lambda_2 = 6.1237$ mm.

III. Investigation of Substrate Resonance Phenomenon

We proceed to investigate the interesting resonance phenomenon arising from the effect of the substrates. The layered structure considered is shown in the inset of the Fig. 5. The substrate used is $LaAlO_3$ with thickness h and no ground plane. The effective surface impedance of the superconducting film at $x = 0$ can be obtained by two successive impedance transformations. The impedance at $x = d$ is given by

$$Z(d) = Z_2 \frac{Z_0 + Z_2 \tanh(jk_2h)}{Z_2 + Z_0 \tanh(jk_2h)}. \tag{8}$$

Consequently, the effective surface impedance at $x = 0$ is expressed as

$$Z_{\text{eff}} = R_{\text{eff}} + jX_{\text{eff}} = Z_1 \frac{Z(d) + Z_1 \tanh(j\tilde{k}d)}{Z_1 + Z(d) \tanh(j\tilde{k}d)} \tag{9}$$

where k_2 is the complex wavenumber in the substrate

$$k_2 = \omega\sqrt{\mu_0\varepsilon_0\tilde{\varepsilon}} \approx \omega\sqrt{\mu_0\varepsilon_0}\sqrt{\varepsilon'}\left(1 - \frac{j}{2}\tan\delta\right) \tag{10}$$

with corresponding propagation constant $\gamma_2 = jk_2 = \alpha_2 + j\beta_2$. Accordingly, the wavelength λ_2 in the substrate at $f = 10$ GHz is directly evaluated as $\lambda_2 = 2\pi/\beta_2 = 6.1237$ mm. Taking a film thickness $d = 5$ nm, and temperature $T = 77$ K, the dependence of R_{eff} on substrate thickness is plotted in Fig. 5 at various reduced static fields. Some features are of interest and worthwhile to note. First, at $b = 0$, which corresponds to Meissner-state response, the resonance (peak) of R_{eff} occurs at the values of h/λ_2 being equal to an odd multiple of quarter wavelengths. In this condition the multilayer structure is equivalent to a lossy transmission line having length of an odd multiple of quarter wavelengths with short-circuited termination. This transmission-line resonator behaves effectively as a parallel lumped-parameter resonant circuit, which makes a maximum R_{eff} at resonance. It is referred to as a short-circuit antiresonance transmission line [26]. Second, at $b \neq 0$, such as $b = 0.05$, the resonance also happens when h/λ_2 is an odd multiple of quarter wavelengths. The resonant peak is, however, a minimum in R_{eff} and more broadened than for $b = 0$. Besides, for $b \neq 0$, the resonance behavior is strongly suppressed at lower b. At the condition of $b \neq 0$, the structure acts as a transmission line with length equal to an odd multiple of quarter wavelengths and an open-circuited termination, implying an equivalent series lumped resonator. Thus, it is similar to the so-called open circuit resonance transmission line [26]. We have so far clearly elucidated two basic lumped resonant circuits which are equivalent to responses for the Meissner-state $(b = 0)$ and the vortex-state $(b \neq 0)$, respectively. The results reveal that a salient resonance phenomenon is expected at higher field in the vortex state. This is well understood from Fig. 3 where the penetration depth increases with increasing b. It will consequently couple more energy to the substrate layer. Therefore, the resonance is more prominent at larger b for a fixed film thickness. Nevertheless, the resonance appears to be less pronounced than $b = 0$. But one should note that for the occurrence of resonance in the mixed state, the substrate contains the maximum energy, whereas it has the least energy in the Meissner-state. For this reason we refer to the parallel circuit as an antiresonator, and the series one as a common resonator. Fig. 6 shows the effective resistance versus h/λ_2 for distinct thicknesses of film at $b = 0$. In order to reach resonance in the substrate, it is naturally required that the penetration depth be larger than the film thickness. It is

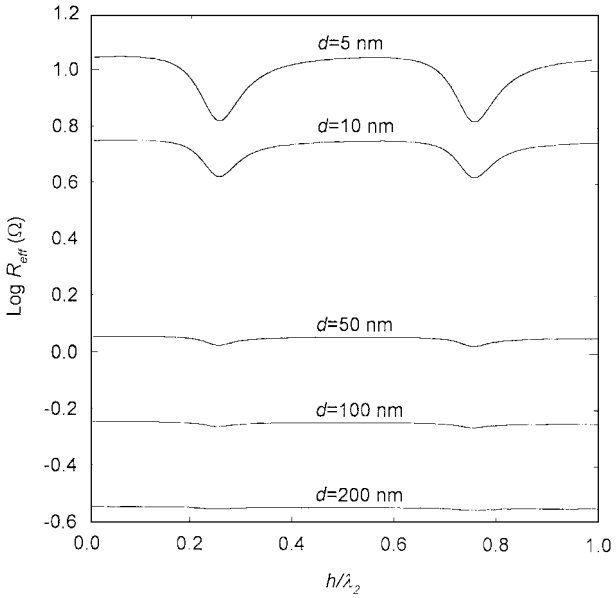

Fig. 7. The effective resistance in (9) versus h/λ_2 for various film thicknesses, $d = 5$ nm, 10 nm, 50 nm, 100 nm, and 200 nm, at $T = 77$ K, 10 GHz, and $b = 0.01$. $\lambda_2 = 6.1237$ mm.

reasonable to conclude that when film thickness increases the observation of resonance becomes less prominent, as shown in Fig. 6. This consequence at $b = 0.1$ is also in Fig. 7. Also, for thicker a film, $d \geq 50$ nm, the resonance behavior is obviously obscure. We thus deduce that the conditions of higher field as well as thinner film would be predominant in observing the interesting resonant results.

The above-mentioned resonant behavior can be further understood on the basis of the so-called transverse resonance technique (TRT) [27]. We now adopt TRT to treat the resonance more carefully. Let us again go back to the structure depicted in the inset of Fig. 5. The impedance of looking backward at $x = d$ is given by

$$Z_b(d) = Z_2 \frac{Z_0 + Z_2 \tanh(jk_2h)}{Z_2 + Z_0 \tanh(jk_2h)}. \tag{11}$$

Similarly, the impedance of looking toward the film at $x = d$ is

$$Z_f(d) = Z_1 \frac{Z_0 + Z_1 \tanh(j\tilde{k}d)}{Z_1 + Z_0 \tanh(j\tilde{k}d)}. \tag{12}$$

The resonance occurs at the condition of

$$Z_b(d) + Z_f(d) = 0 \tag{13}$$

according to the TRT. In order to self-consistently check the results given in Fig. 5, we again take $d = 5$ nm for the film thickness and temperature, $T = 77$ K. By treating the substrate thickness h as a parameter we can solve (13) for angular frequency ω. Listed below are three arbitrary conditions for illustrative purpose.

a) $b = 0$: $\omega = 63.1639 + j8.3253(\text{GHz})$, when $h = \frac{1}{4}\lambda_2$,
$\omega = 62.9423 + j2.7655(\text{GHz})$, when $h = \frac{3}{4}\lambda_2$,
$\omega = 62.8982 + j1.6582(\text{GHz})$, when $h = \frac{5}{4}\lambda_2$.

b) $b = 0.01$: $\omega = 61.8782 + j13.9441(\text{GHz})$, when $h = \frac{1}{4}\lambda_2$,
$\omega = 62.5417 + j4.6704(\text{GHz})$, when $h = \frac{3}{4}\lambda_2$,
$\omega = 62.6608 + j2.8051(\text{GHz})$, when $h = \frac{5}{4}\lambda_2$.

c) $b = 0.05$: $\omega = 62.2263 + j42.5273(\text{GHz})$, when $h = \frac{1}{4}\lambda_2$,
$\omega = 62.6312 + j14.2665(\text{GHz})$, when $h = \frac{3}{4}\lambda_2$,
$\omega = 62.7116 + j8.5709(\text{GHz})$, when $h = \frac{5}{4}\lambda_2$.

The solutions for ω in (13) implicitly include much information about the resonance phenomenon. First, the introduction of complex angular frequency is not surprising in that (13) is mathematically a complex-number equation. The real part of ω is the real resonant frequency, which is in fairly good agreement with the observation in Fig. 5 where we have chosen the frequency as 10 GHz, corresponding to 62.8318 GHz in angular frequency. The imaginary part of ω, however, represents the loss in the resonant structure. Moreover, the higher ω, the greater the loss. Second, looking at the results of $b = 0$, it is interesting to see that the magnitude of the imaginary part decreases with increasing h, implying lower loss in the thicker substrate. This phenomenon is attributed to the fact that shunt conductance is inversely proportional to the thickness of the parallel-plate transmission line, that is, the substrate thickness h. Therefore, the increase of h will decrease the conductance loss, which agrees with the results obtained for the imaginary part of the complex frequency. A similar argument also holds when $b \neq 0$. Regarding the real component of the complex frequency, it shows no significant variation for the three respective conditions considered.

In Fig. 8, the temperature-dependent effective surface resistance displays an oscillating behavior which is very similar to the observation in the normal state as reported in the work of Drabeck *et al.* [10]. The substrate used is $SrTiO_3$ with permittivity $\varepsilon(T) = c_1/[\coth(T_0/T) - c_2]$, where $c_1 = 2.14 \times 10^3, c_2 = 0.905$, and $T_0 = 42$ K [10]. To compare the oscillating behavior in the normal state as observed by Drabeck *et al.* [10], [11], Fig. 8 has been obtained from their conditions, i.e., the thicknesses of the film and substrate are $d = 600$ nm and $h = 1$ mm, respectively, and the frequency is 100 GHz. In addition, we take the reduced field as $b = 0.05$.

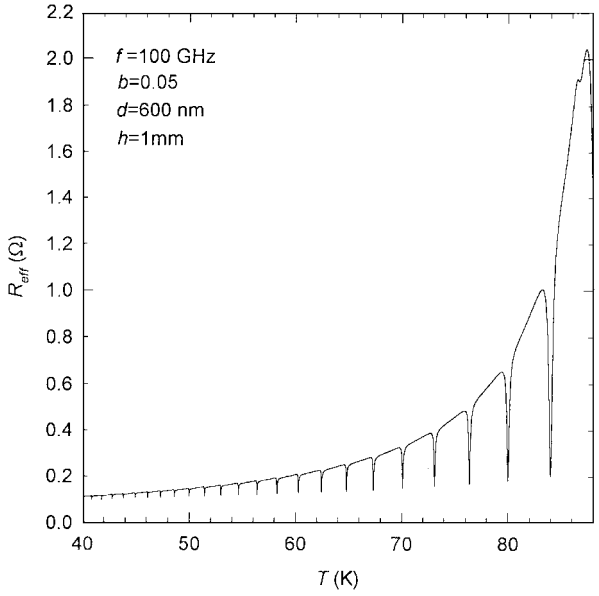

Fig. 8. The effective surface resistance in (9) as a function of temperature, at $f = 100$ GHz, $b = 0.05, d = 600$ nm, and $h = 1$ mm.

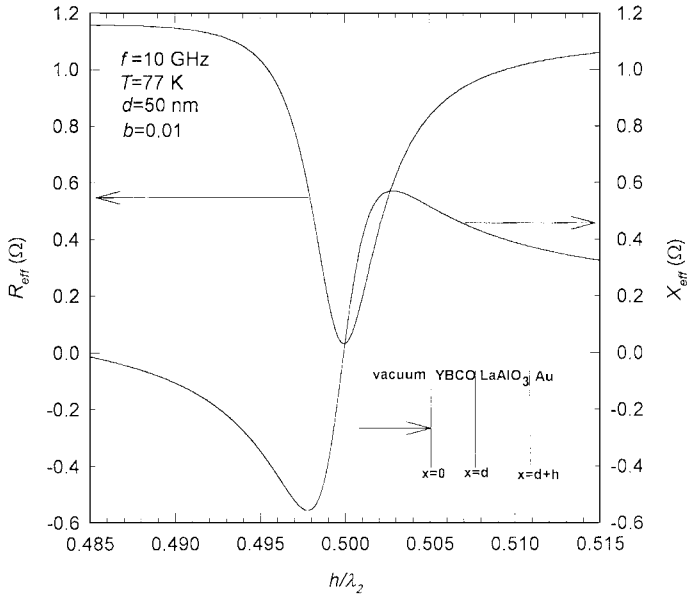

Fig. 9. The effective surface resistance and reactance versus h/λ_2 around the resonance point. The conditions are given in the figure. The material parameters are given in the text.

As can be seen, the oscillation amplitude increases rapidly with increasing temperature, especially near T_c. The rising rate of amplitude is greater than that in the normal state, see Fig. 1 in [10]. This oscillation phenomenon is due to standing waves confined in the substrate and is closely related to the highly temperature-dependent permittivity of $SrTiO_3$. Besides, the oscillation is not seen when $b = 0$. It indicates that the inclusion of vortices has increased the oscillation because of the high resistance from vortex motion.

Finally, we examine the resonant structure where a ground metal, gold ($\sigma_m = 4.1 \times 10^7$ S/m) is deposited at the backside of the substrate. The effective microwave surface impedance is again described in (8), (9), and (10), but we replace Z_0 in

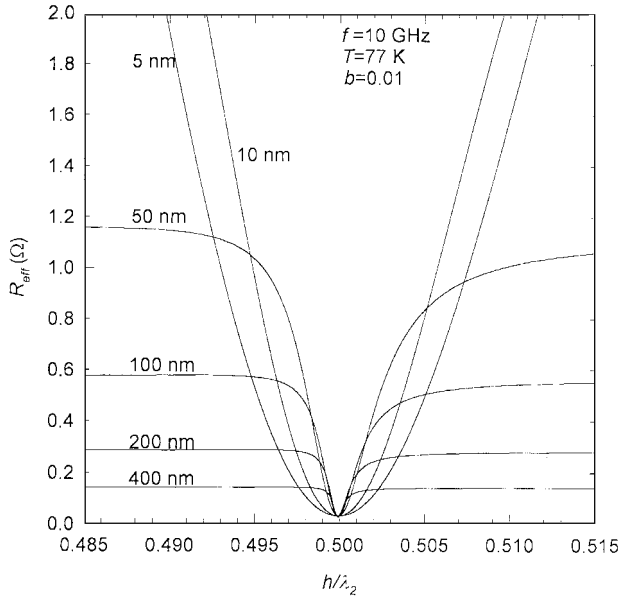

Fig. 10. The effective surface resistance versus h/λ_2 for different film thickness, $d = 5$ nm, 10 nm, 50 nm, 100 nm, 200 nm, and 400 nm. The conditions and parameters are the same as in Fig. 8.

(8) by Z_3, where $Z_3 = \sqrt{j\omega\mu_0/\sigma_m}$ is the wave impedance of the ground metal. The resonant behavior is now inspected around the value of $h = \lambda_2/2$, as shown in Fig. 9. Here, the conditions considered are $f = 10$ GHz, $T = 77$ K, $h = 50$ nm, and $b = 0.01$. The addition of the ground metal has greatly increased the magnitude of R_{eff} as compared with Fig. 7 and enhanced the resonance as well. Another change made is the occurrence of a resonance when h/λ_2 equals a multiple of half-wavelength. It now acts as a transmission line with length, $l = n(\lambda_2/2), n = 0, 1, 2, \cdots$, and short-circuit termination, or a series lumped resonant circuit. The reactance shows an abrupt change from capacitive to inductive around the resonance point. The result shown in Fig. 9 is a key feature about resonance, which is quite analogous to the resonance spectra of anomalous dispersion characteristics of the complex permittivity of dielectrics [28]. In Fig. 10, we plot the R_{eff} versus h/λ_2 for various thicknesses of film for the same conditions as in Fig. 9. The effect of film thickness on resonance is basically similar to that in Fig. 7. However, the suppression of resonance for a thick film is not as severe as in Fig. 7, which in turn indicates that the ground metal has a positive influence on the appearance of resonance. It is also of interest to note that the resonance position is not shifted due to the variation of the film thickness. This observation is quite different from that in the Meissner state shown in the work of Hartemann [12]. In the Meissner state the increase of film thickness not only lowers the resonance peak but also moves the peak position to the right, an increase of ratio h/λ_2. This suggests a basic difference in the dependence of resonance on film thickness between mixed and Meissner states.

IV. Summary

The study of effective microwave surface impedance is important for microwave applications and also for understanding

the fundamental physics of high-T_c superconductors. Aided by the Coffey–Clem model, in addition to transmission line theory, we have systematically examined the effective surface impedance of HTSC in the mixed state. In a nonresonant structure the effective surface impedance has been investigated as a function of film thickness and static field. The possible influence of substrate material on impedance is also considered. Our results demonstrate that the field-dependent critical film thickness for shielding the substrate increases with increasing static field. This fact is clearly elucidated in light of field-dependent complex RF penetration depth.

Considering the resonant structures, we find a very fundamental distinction between the Meissner and mixed-state responses. In the Meissner state, the layered structure acts as an antiresonant transmission line or, equivalently, a lumped parallel resonator when the backside of the substrate is vacuum. However, it behaves like a lumped series resonant circuit in the mixed state. The switching from parallel to series, or vice versa, is closely connected with the strong difference in the wave impedances of distinct states. The resonant phenomenon is further well described by the transverse resonance technique. Results indicate that the thin film will be a preference for obtaining the resonance. By adding the ground metal at the backside of the substrate, the resonant behavior is highly enhanced together with a shift of one quarter-wavelength in peak position. It is of practical interest to understand the distinctions associated with the resonance phenomenon. The results given here strongly suggest that for microwave applications, attention should be given to this phenomenon.

REFERENCES

[1] S. H. Talisa, M. A. Janocko, C. Moskowitz, J. Talvacchio, J. F. Billing, R. Brown, D. C. Buck, C. J. Jones, B. R. McAvoy, G. R. Wanger, and D. H. Watt, "Low- and high-temperature superconducting microwave filters," *IEEE Trans. Microwave Theory Tech.*, vol. 39, pp. 1448–1454, 1991.

[2] C. Wilker, Z. Y. Shen, P. Pang, D. W. Face, W. L. Holstein, A. L. Matthews, and D. B. Laubacher, "5 GHz High-temperature-superconductor resonators with high Q and low power dependence up to 90 K," *IEEE Trans. Microwave Theory Tech.*, vol. 39, pp. 1462–1467, 1991.

[3] H. How, R. G. Seed, C. Vittoria, D. B. Chrisey, J. S. Horwitz, C. Carosella, and V. Folen, "Microwave characteristics of high T_c superconducting coplanar waveguide resonator," *IEEE Trans. Microwave Theory Tech.*, vol. 39, pp. 1668–1673 1991.

[4] J. M. Pond, J. H. Claassen, and W. L. Carter, "Measurements and modeling of kinetic inductance microstrip delay lines," *IEEE Trans. Microwave Theory Tech.*, vol. MTT-35, pp. 1256–1262, 1987.

[5] H. Piel and G. Muller, "The Microwave surface impedance of high-T_c superconductors," *IEEE Trans. Magn.*, vol. 27, pp. 854–862, 1991.

[6] G. Muller, N. Klein, A. Brust, H. Chaloupka, M. Hein, S. Orbach, H. Piel, and D. Reschke, "Survey of microwave surface impedance data of high-T_c superconductors-evidence for nonpairing charge carriers," *J. Superconduct.*, vol. 3, pp. 235–242, 1990.

[7] Y. Kobayashi and T. Imai, "Phenomenological description of conduction mechanism of high-T_c superconductors by three-fluid model," *IEICE Trans.*, vol. E74, pp. 1986–1992, 1991.

[8] Y. Kobayashi, T. Imai, and H. Kayano, "Microwave measurement of temperature and current dependences of surface impedance for high-T_c superconductors," *IEEE Trans. Microwave Theory Tech.*, vol. 39, pp. 1530–1538, 1991.

[9] N. Klein, H. Chaloupka, G. Muller, S. Orbach, H. Piel, B. Roas, L. Schultz, U. Klein, and M. Peiniger, "The effective microwave surface impedance of high-T_c thin films," *J. Appl. Phys.*, vol. 67, pp. 6940–6945, 1990.

[10] L. Drabeck, K. Holczer, and G. Gruner, "Ohmic and radiation losses in superconducting films," *J. Appl. Phys.*, vol. 68, pp. 892–894, 1990.

[11] L. Drabeck, K. Holczer, G. Gruner, J. J. Chang, D. J. Scalapino, and T. Venkatesan, "An experimental investigation of $YBa_2Cu_3O_7$ films at millimeter-wave frequencies," *J. Superconduct.*, vol. 3, pp. 317–322, 1990.

[12] P. Hartemann, "Effective and intrinsic surface impedances of high-T_c superconducting thin films," *IEEE Trans. Appl. Superconduct.*, vol. 2, pp. 228–235, 1992.

[13] D. E. Oates, A. C. Anderson, C. C. Chin, J. S. Derov, G. Dresselhaus, and M. S. Dresselhaus, "Surface-impedance measurements of superconducting NbN films," *Phys. Rev. B, Condens. Matter*, vol. 43, pp. 7655–7663, 1991.

[14] A. Mogro-Campero, L. G. Turner, A. M. Kadin, and D. S. Mallory, "Film thickness dependence of microwave surface resistance for $YBa_2Cu_3O_7$ thin films," *J. Appl. Phys.*, vol. 73, pp. 5295–5297, 1993.

[15] R. Pinto, A. G. Chourey, and P. R. Apte, "Effective surface resistance of $LuBa_2Cu_3O_{7-x}$ thin films," *Appl. Phys. Lett.*, vol. 64, pp. 2166–2168, 1994.

[16] T. Kuhlemann and J. H. Hinken, "Measurements of the thickness dependence of the surface resistance of laser ablated high-T_c superconducting thin films," *IEEE Trans. Magn.*, vol. 27, pp. 872–875, 1991.

[17] N. Klein, G. Muller, S. Orbach, H. Piel, H. Chaloupka, B. Roas, L. Schultz, U. Klein, and M. Peiniger, "Millimeter wave surface resistance and London penetration depth of epitaxially grown $YBa_2Cu_3O_{7-x}$ thin films," *Physica C*, vol. 162–164, pp. 1549–1550, 1989.

[18] M. W. Coffey and J. R. Clem, "Unified theory of effects of vortex pinning and flux creep upon the RF surface impedance of type-II superconductors," *Phys. Rev. Lett.*, vol. 67, pp. 386–390, 1991.

[19] J. R. Clem and M. W. Coffey, "Effects of flux flow, flux pinning, and flux creep upon the RF surface impedance of Type-II superconductors," *J. Superconduct.*, vol. 5, pp. 313–318, 1992.

[20] M. W. Coffey and J. R. Clem, "Theory of RF Magnetic permeability of isotropic type-II superconductors in a parallel field," *Phys. Rev. B, Condens. Matter*, vol. 45, pp. 9872–9881, 1992.

[21] M. W. Coffey and J. R. Clem, "Theory of microwave transmission and reflection in type-II superconductors in the mixed state," *Phys. Rev. B, Condens. Matter*, vol. 48, pp. 342–350, 1993.

[22] E. K. Moser, W. J. Tomasch, J. K. Furdyna, M. W. Coffey, and J. R. Clem, "Transmission and reflection of superconducting $YBa_2Cu_3O_{7-x}$ films at 35 GHz," *IEEE Trans. Appl. Superconduct.*, vol. 3, pp. 1119–1122, 1993.

[23] J. Owliaei and S. Sridhar, "Field-dependent crossover in the vortex response at microwave frequencies in $YBa_2Cu_3O_{7-x}$ Films," *Phys. Rev. Lett.*, vol. 69, pp. 3366–3369, 1992.

[24] M. S. Pambianchi, D. H. Wu, L. Ganapathi, and S. M. Anlage, "DC magnetic field dependence of the surface impedance in superconducting parallel plate transmission line resonators," *IEEE Trans. Appl. Superconduct.*, vol. 3, pp. 2774–2777, 1993.

[25] S. Revenaz, D. E. Oates, D. Labbe-Lavigne, G. Dresselhaus, M. S. Dresselhaus, "Frequency dependence of the surface impedance of $YBa_2Cu_3O_{7-x}$ thin films in a DC magnetic field: investigation of vortex dynamics," *Phys. Rev. B, Condens. Matter*, vol. 50, pp. 1178–1189, 1994.

[26] R. E. Collin, *Foundations For Microwave Engineering*, 2nd eds. New York: McGraw-Hill, 1992.

[27] D. M. Pozar, *Microwave Engineering*. Reading, MA: Addison-Wesley, 1993.

[28] A. von Hippel, *Dielectrics and Waves*. Norwood, MA: Artech House, 1995.